The Influence of Sand Grain Strips on Boundary Layer Transition in the Towing Tank

Copyright © **Ulrich Remmlinger**, Germany, November 2013

Abstract. Based on a literature survey the paper provides equations for engineering calculations of the tripped transitional boundary layer with sand grain strips. Typical applications are ship model hulls in a towing tank.

NOMENCLATURE

A_S	Free surface between the grains, per grain		x	Distance on the surface downstream from forward stagnation point
c_f	friction coefficient = $drag\ force\ / (\rho/2 \cdot U_\infty^2 \cdot area)$			
f_{tr}	Linear combination factor in transition zone		γ	Intermittency factor
H	Shape factor θ/δ^*		δ	Thickness of b. l. at $u/U = 0.99$
k	Height of the roughness particle		δ^*	Displacement thickness of b. l.
L_{WL}	Length of waterline		θ	Momentum thickness of b. l.
Re_x	Reynolds number $U_\infty \cdot x / v$		ρ	Density
Re_θ	Reynolds number $U \cdot \theta / v$		v	Kinematic viscosity
Re_k	Reynolds number $u_k \cdot k / v$			
Tu	Turbulence level in %		Subscripts:	
u	Velocity within the boundary layer			
U	Velocity at the edge of the b. l.		k	at the top of the particle
U_∞	Undisturbed velocity in front of the body		lam	for laminar flow
V_R	Volume of the roughness particle		$turb$	for turbulent flow
			0	at location of trip

1. INTRODUCTION

A ship model that is tested in the towing tank at the design Froude number will be run at such a low Reynolds number, that the boundary layer is in the laminar state on the forward half of the hull. Since in the full size ship the b.l. will turn turbulent almost immediately behind the bow, viscous effects will not be modeled correctly. To overcome this deficit, the b.l. is often artificially tripped near the bow in the hope, that the resulting turbulent b.l. behaves similar to the one along the full size ship. The tank tests of the Delft Systematic Yacht Hull Series were all conducted using small strips of carborundum sand for a b.l. trip [1]. These tests form a huge and valuable database that can be used for resistance predictions of sailing yachts. To extrapolate the measured resistance to full scale using Froude's method, the viscous resistance of the model must be known. The size and the position of the sand grain strips have a significant influence on the state of the b.l. and hence on the viscous resistance. The viscous resistance of the model hull where the b.l. is tripped at the bow can be twice as high as the resistance of the same hull with natural transition. The data of the DSYHS can therefore only be used correctly if the influence of the sand grain strips is known in detail. The following literature survey is conducted to find a simplified model for engineering calculations, not to investigate the complex physics of turbulent flows.

The effect of various methods of stimulating transition in the boundary layer on a tanker model in the towing tank was studied by Breslin and Macovsky [2] already in 1950 with the help of the hot-wire method. The results indicated that the nature of the b.l. behind a trip wire and behind a sand grain strip differ substantially. Klebanoff et al. [3] showed the fundamentally different character of the two-dimensional disturbances behind a trip wire and the turbulent wedge behind a three-dimensional roughness element on a flat plate in the wind tunnel. Since our task is the analysis of the DSYHS data, the following study will be limited to the influence of the three-dimensional roughness. The roughness element acts as an obstacle in the flow that causes a horseshoe-vortex on the wall in front and hairpin-vortexes with their ends normal to the wall, close to the separation lines, at the rear side of the obstacle. The transition of the flow from laminar to turbulent occurs due to wake instability and vortex shedding behind the roughness element. The linear instability mechanism of the b.l. is by-passed.

Braslow et al. [4] reported that there is a minimum grain height to start the transition to turbulent flow. This minimum height is a function of the local Reynolds number and the thickness of the b.l.. Smaller grains have no influence and the flow will remain laminar. Braslow gives for aircraft wings the numerical value of 600 for Re_k, the Reynolds number based on the grain size that would initiate transition. This value is valid beyond the local Reynolds number $Re_x = 1.5 \cdot 10^5$. Closer to the leading edge the necessary grain size is larger, numerical values

are not given. Klebanoff et al. [5] measured values for Re_k of 325 for hemispheres and 450 for cylindrical elements. In a review of the literature they found values for Re_k as low as 45 for flat triangles and up to 1000 for cylindrical elements.

Detailed experiments, including hot wire anemometry, were conducted by Doenhoff and Horton [6] on a NACA 65(215)-114 airfoil. This airfoil has a favorable pressure gradient up to 50% of its chord. The velocity distribution is similar to the flow along the hull of a sailing yacht, were the maximum velocity can also be found at the midship section. Doenhoff and Horton report the phenomenon that the flow is identical to the laminar flow over a smooth surface if the grain size is not large enough to initiate the transition, i.e. the flow does not "memorize" the roughness strip. They also found that the transition depends only on the conditions at the downstream end of the roughness strip; the streamwise extent of the strip had no effect. Kerho and Bragg [7] support this with measurements on a NACA 0012 airfoil with different locations and extents of the roughness strips. This opens up the opportunity to make use of test results gained on rough surfaces in general with the roughness starting at the leading edge and the relevant database is not only limited to small strips of roughness. The independence on the extent is of course only valid for the initiation of the transition, not for the magnitude of the drag.

2. CRITICAL REYNOLDS NUMBER UNDER THE INFLUENCE OF ROUGHNESS

Newer test results on rough surfaces make it possible to replace Braslow's "rule of thumb" with a more detailed computation of the critical Reynolds number at transition onset. An empirical correlation of more than 400 test results was lately reported by Lorenz et al. [8]. The tests were made in the stator of a gas turbine cascade, which is a flow situation with a mild favorable pressure gradient because the flow is accelerated. The outcome is a correlation for the b.l. momentum thickness that is required to trigger the transition. The input variables are the roughness height and density, the b.l. displacement thickness and the turbulence level of the free stream. The pressure gradient along the surface is not considered.

2.1 Equations of the empirical correlation

The geometric roughness height is converted into an effective height using the following equations:

$$\Lambda_R = \frac{k \cdot A_S}{V_R}$$

$$k_{eff} = k \cdot 1.35 \cdot \left(1 - \frac{1}{\Lambda_R}\right) \cdot \Lambda_R^{-0.28}$$

(1)

For $k_{eff} > 0.01 \cdot \delta^*$ the roughness has an effect on the critical momentum thickness:

$$Re_{\theta,crit,rough} = \left(\frac{1}{Re_{\theta,crit,smooth}} + 0.00937 \cdot f_{rough}\right)^{-1}$$

(2)

The roughness function is computed from the following equations:

$$f_{rough} = \exp(-k_\delta) \cdot (k_\delta - 0.01)^\alpha + (1 - \exp(-k_\delta)) \cdot (k_\delta - 0.01) \cdot C$$

$$\alpha = \min(0.4 \cdot Tu + 0.8, 3.0)$$

$$C = 0.1 \cdot Tu + 0.85$$

$$k_\delta = \frac{k_{eff}}{\delta^*}$$

(3)

Lorenz et al. use for the critical momentum Reynolds number over smooth surfaces an own correlation that depends only on the turbulence level. It might be better to use the well established correlation by Abu-Ghannam and Shaw [9] which also takes into account the pressure gradient. A slight modification by Fraser et al. [10] adapts the A-G&S correlation to the more recent test results:

$$Re_{\theta,crit,smooth} = 0.85 \cdot \left(163 + \exp\left(g(m) \cdot \left(1 - \frac{Tu}{6.91} \right) \right) \right)$$

$$g(m) = 6.91 + 12.75 \cdot m + 63.64 \cdot m^2 \quad \text{for} \quad m < 0$$

(4)

$$g(m) = 6.91 + 2.48 \cdot m - 12.27 \cdot m^2 \quad \text{for} \quad m > 0$$

$$m = \frac{\theta^2}{\nu} \cdot \frac{dU}{dx}$$

The parameter range for the correlation was $Tu = 0.2 - 15.7$ % and $k/\delta^* = 0.1 - 6.3$. The procedure is now as follows:

1. determine geometry and amount per area of the roughness particles, calculate k_{eff} from eq. 1
2. calculate the properties of the laminar boundary layer without roughness, starting at the forward stagnation point and continue downstream to the rear end of the sand grain strip
3. calculate $Re_{\theta,\,crit,\,rough}$ for this location, using eq. 2-4
4. compare Re_θ from step 2 with the critical value from step 3. If the critical value is exceeded, the transition of the b.l. will begin. If Re_θ is less than the critical value, the b.l. will remain laminar and the sand grain strip is non-existent for the flow.

To check the validity of the calculation method, the procedure is applied to the cases described in [6] and [7]. The boundary layer calculation required in step 2 is performed with the program XFOIL [11].

2.2 Comparison with test results of a NACA 0012 airfoil

The roughness elements used by Kerho and Bragg [7] were staggered hemispherical shapes glued onto a substrate. The height above the substrate was 0.25 mm. The center to center spacing was 1.3 mm. This geometry
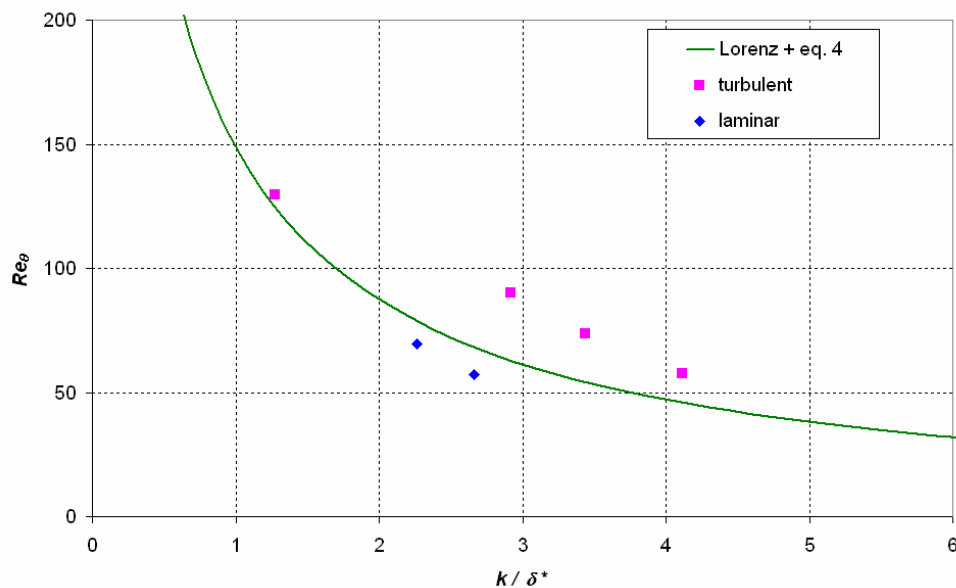
Figure 1. Momentum Reynolds number at the roughness strips of a NACA 0012 airfoil

gives a value of 11.4 for Λ_R. For the roughness positions close to the critical values, the results are depicted in figure 1. Kerho and Bragg did not determine the exact critical Reynolds number; they just measured whether the b.l. behind the roughness strip was laminar or turbulent. Lorenz's correlation line for the critical Reynolds number successfully separates the turbulent and laminar cases. This is a helpful result, because the roughness strips are so close to the leading edge that Braslow's rule would not be applicable ($Re_x < 0.5 \cdot 10^5$). The usage of eq. 4 is necessary to correctly identify the turbulent status for the case of $k/\delta^* = 1.28$. If instead the critical momentum Reynolds number over smooth surfaces as proposed by Lorenz were used, laminar flow would have been predicted.

2.3 Comparison with test results of a NACA 65(215)-114 airfoil

Doenhoff and Horton [6] used grit No. 60 carborundum grains, cemented to the surface by a thin coat of shellac. The density is only approximately given with 500 – 1000 grains per sq. in.. The same sandpaper type b.l. trips were used by Braslow and a more detailed description, including a histogram of the grain sizes, is given in [4]. A close up photograph can be found in [12]. From this information an average grain size of 0.0112 inch and a density of 724 grains per sq. in. can be deduced. If we assume that the lowest 20% of each grain are buried in the shellac we get $k = 0.228$ mm and $\Lambda_R = 13.6$. The critical Reynolds numbers for the start of transition, calculated and measured, are shown in figure 2. Considering the fact that k/δ^* is outside of the correlated parameter range, the prediction seems to be acceptable. The discrepancy of 50% at $k/\delta^* = 10$ is large, but Braslow's rule would be 100% off at the lower end and would not be applicable for the higher values of k/δ^*.
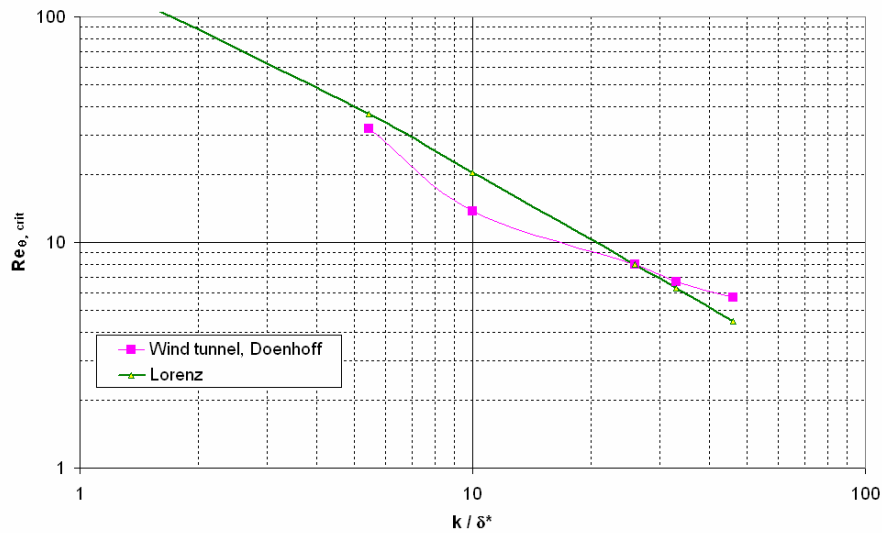
Figure 2. Critical momentum Reynolds number at the roughness strips of a NACA 65(215)-114 airfoil

2.4 Comparison with test results of a cylinder

In the two previous test cases the roughness height was larger than the displacement thickness of the b.l.. We now need to know if Lorenz's correlation also works for smaller roughness heights. The range below $k/\delta^* < 1$ was investigated by Feindt [13] on a cylinder, longitudinally placed in a closed wind tunnel with several different, but constant pressure gradients applied. The cylinder was covered with commercially available sand
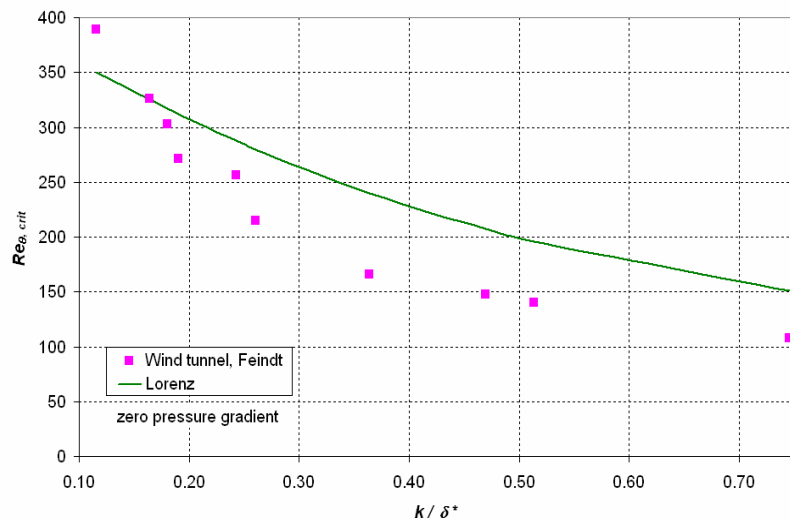
Figure 3. Critical momentum Reynolds number without pressure gradient, surface with No. 60 grit

paper. The No. 60 grit has a density of 2200 grains per sq. in., which is much higher than in the previous example. Λ_R decreases down to 6.1. The comparison of calculated and measured critical Reynolds number in figure 3 is somewhat disappointing. The suction in front of the leading edge of the sandpaper that is necessary to remove the incoming b.l. might have had an influence. The suction rate was kept constant and was not individually adjusted. The maximal error is 45% for the higher k/δ^*. Feindt also measured the influence of a constant non-zero pressure gradient in the wind tunnel on the critical Reynolds number. Figure 4 shows the comparison between measured and computed values. In the ideal case the symbols would lie on the diagonal line. The maximal error is 16%. It is obvious that the inclusion of the pressure gradient in equation 4, in the form proposed by A-G&S, improves the prediction compared to Lorenz's original paper.

$$\frac{dp}{dx} = 0.745 \cdot \frac{\rho}{2} \cdot U_\infty^2$$
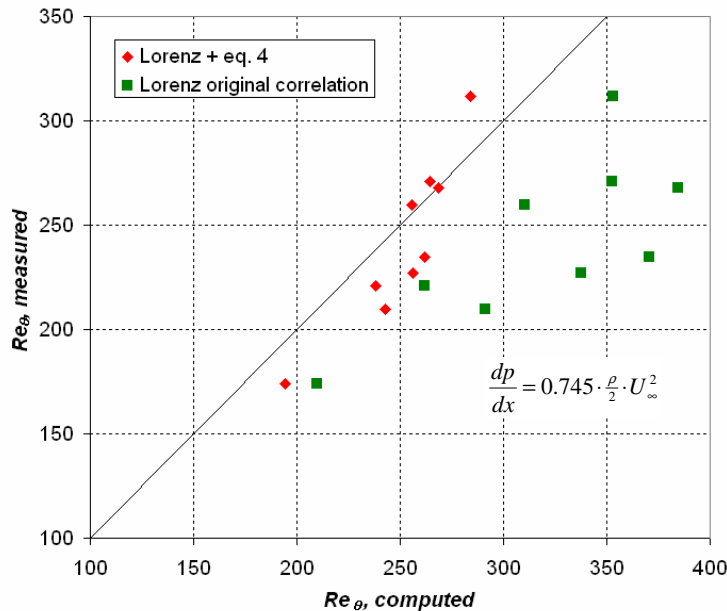
Figure 4. Critical momentum Reynolds number in retarded flow grit No. 60-220

Finally Feindt provided results for an accelerated flow with a constant negative pressure gradient. Figure 5 compares measurements and prediction. The maximal error is -14%.

$$\frac{dp}{dx} = -0.487 \cdot \frac{\rho}{2} \cdot U_\infty^2$$
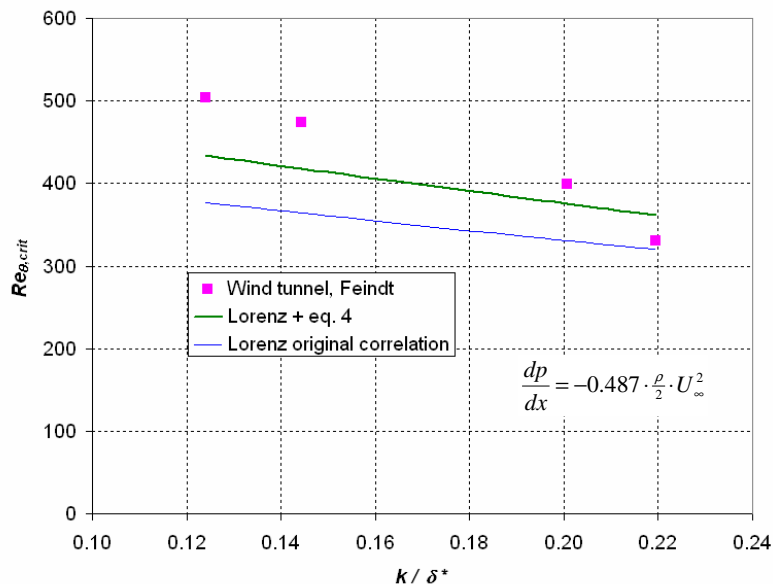
Figure 5. Critical momentum Reynolds number in accelerated flow, grit No. 60-220

In summary one can say that the predicted transition Reynolds numbers are only approximate, but still better than all previously proposed approximations. Braslow's rule was developed for wind tunnels with extremely low turbulence levels. As Feindt's measurements were conducted at a turbulence level of 1.2%, Braslow's rule fails under these circumstances. At the measured transition location Re_k reaches only values between 40 and 200, which is far less than the threshold of 600 that would indicate transition to turbulence according to his rule.

The early work of Klebanoff et al. [3] can not directly be compared to Lorenz's correlation, because they investigated a special phenomenon of the single row of spheres. The wedge of sustained turbulence behind the sphere begins at a certain distance downstream from the element. When the wind speed in the tunnel is increased, the apex of the wedge moves upstream and finally reaches the sphere. Klebanoff et al. [3] give the Reynolds number for this "attached" condition. Compared to Lorenz's prediction of $Re_{\theta, crit}$ for the first sustained turbulence, the values calculated for the attached condition [3] are consistently 2.4 times higher.

3. TRANSITION ZONE

The measurements of Kerho and Bragg [7] show that the transition zone behind a b.l. trip can be significantly longer than in the case of natural transition. It takes a certain distance and time for the turbulent spots to grow and merge and to develop into fully turbulent flow. If the b.l. calculation along the ship's hull were switched from the laminar to the turbulent equations at the transition point, the overall viscous resistance could be seriously overestimated. It is therefore necessary to know the length of the transition zone and in addition a method is required that allows the calculation of the skin friction coefficient and the b.l. thickness in this zone.

3.1 Transition length

An explicit investigation of the transition length ΔRe_x is reported in [14]. Gibbings et al. come to the conclusion, that the length of the transition zone can be correlated to the value of the Reynolds number Re_x at the location of the b.l. trip. Figure 6 shows this correlation for all available data. Since the transition length varies by two orders of magnitude for an identical value of Re_x, this seems not to be a realistic correlation.
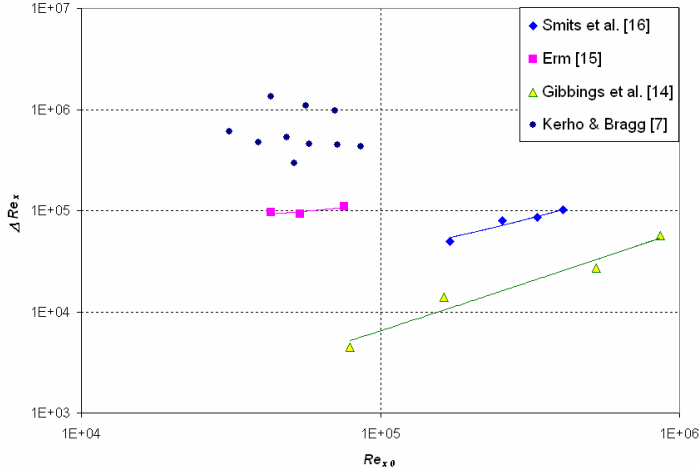
Figure 6. Transition length as a function of the Reynolds number at the location of the trip
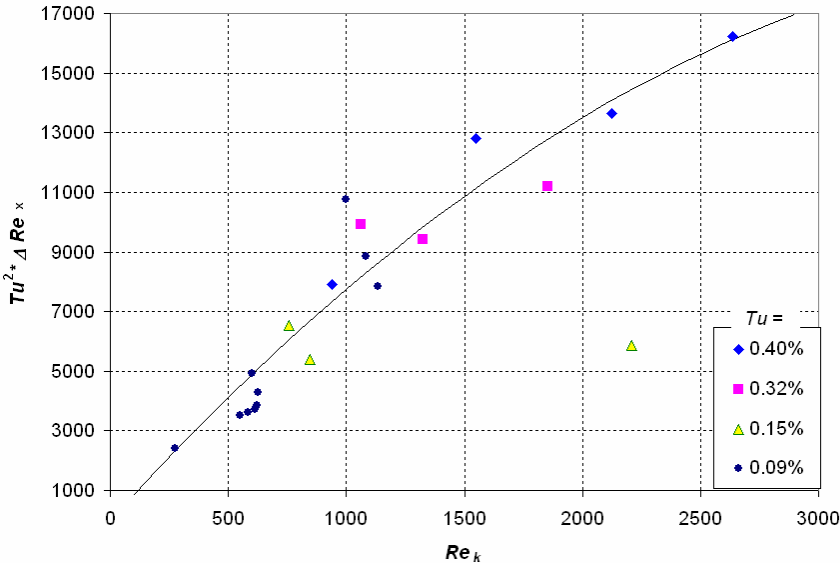
Figure 7. Transition length $\cdot Tu^2$ as a function of Re_k

The experimental results in figure 6 were gained in different wind tunnels at different turbulence levels, so Tu has obviously to be taken into account. For natural transition Fransson et al. [17] demonstrate, that the transition length is proportional to $1/Tu^2$. Further information can be found in [5]; Klebanoff et al. argue that the transition length will most likely depend on Re_k. These statements lead to the correlation that is depicted in figure 7. In this diagram the transition length of the experiments by Gibbings et al. [14] was taken from their diagram of the shape factor, as Re_k is given only for this data. Their b.l. trip consists of balls on a flat plate. Kerho and Bragg [7] used a NACA 0012 airfoil for their experiments with hemispherical roughness elements. The tests by Erm [15] and Smits et al. [16] were conducted with flat plates at zero pressure gradients; a row of cylindrical studs was used for the b.l. trip. The relative roughness height k/δ varied between 0.3 and 1.5 in the experiments depicted in figure 7. From natural transition it is known, that the pressure gradient has an influence on the transition length and most likely this is also the case for the tripped transition, but the available data is presently insufficient for such an analysis. Considering the different experimental configurations in figure 7, including the NACA 0012 with a pressure gradient, the correlation seems to be acceptable for engineering calculations. The curve drawn in the diagram follows the equation:

$$\Delta Re_x \cdot Tu^2 = 8.75 \cdot Re_k - 0.001 \cdot Re_k^2 \tag{5}$$

It is interesting to note, that even in the early measurements by Breslin and Macovsky [2] the influence of the turbulence level is visible. As a result of the increased turbulence induced by the breaking bow wave, the transition length close to the water surface is much shorter than down below.

3.2 Transition model

There are several models for the b.l. calculation in the transition zone with natural transition. An overview is given by Narasimha [18], more recent results can be found in [17] and [19]. A successful approach is the linear combination of a laminar and a turbulent velocity profile. The idea reflects the fact, that at a given point in space the flow alternates in time between a laminar flow and a turbulent spot. The time share, during which the turbulent fluctuations are present, is called intermittency factor γ. The value of 1 describes the fully turbulent flow and 0 the undisturbed laminar flow. For details about the variation of γ see [20]. The linear combination allows calculating the properties of the transitional b.l. The calculation of the laminar flow starts at the forward stagnation point. The turbulent properties are calculated for a fully turbulent flow that starts upstream of the transition point. The starting point is determined by the condition that the turbulent b.l. thickness δ at the transition point matches the value of the laminar case. In the transition zone the two velocity profiles are linearly combined. The following equation is used e.g. for the skin friction coefficient:

$$c_f = f_{tr} \cdot c_{f,turb} + (1 - f_{tr}) \cdot c_{f,lam} \tag{6}$$

In case of natural transition, the linear combination factor f_{tr} is identical to the intermittency factor γ. The displacement thickness can be calculated in the same way as c_f, the momentum thickness requires a more complex calculation [21].

It is an open question, whether this model, that successfully describes the natural transition, can also be used in the case of a tripped b.l. The Reynolds number in the transition zone is much lower in the tripped case and the turbulent velocity profile that is needed for the linear combination might not exist at these low Re_θ values. Valuable information is given by Park et al. [22] as a result of their numerical simulation. The distributions of the turbulence properties within an individual turbulent spot at $Re_\theta = 300$ closely resemble the properties in the developed turbulent state at $Re_\theta = 1840$. Even if the turbulence is not sustained, which is the case if only turbulent spots appear over a short time, the friction coefficient within these turbulent spots can be calculated by extrapolating the 1/7 power-law approximation down to low Reynolds numbers. In a similar manner Spalart [23] studied the flow at low Reynolds numbers by direct simulation and concluded that in sustained turbulence the wall and wake regions begin to overlap at Re_θ lower than 400, with the consequence that the logarithmic layer disappears. Therefore a classical "fully developed" turbulent flow does not exist below $Re_\theta = 400$, but the velocity profile can be approximated by a power law. Smits et al. [16] came to slightly different results, when they measured the tripped turbulent b.l. behind a row of pins in the wind tunnel. Even at $Re_\theta = 354$ for zero pressure gradient and at 261 for a strong favorable pressure gradient flow, they found a logarithmic region in the velocity profiles. Nevertheless the skin friction coefficient could be fitted well by a simple 1/7 power-law approximation. Their approximation with an additional correction for the turbulence level according to Stefes [24] will be used for the determination of $c_{f,turb}$ within the transition zone.

Finally we need an equation for the calculation of f_{tr} as a function of the distance from the tripping device. As already indicated, for a tripped b.l. the value of the factor f_{tr} is not equivalent to the intermittency factor as in the

case of natural transition. The reason for this discrepancy is the region of separated flow behind the obstacle. The turbulent fluctuations and therefore the intermittency factor are high because of the vortex shedding, whereas the shear-stress at the wall is low and can even become negative in the recirculating flow region. The experimental results in [5] illustrate this situation for a single roughness element. The momentum thickness in figure 8 is a copy from [5], with the curves for the laminar and turbulet b.l. added. The momentum equation for 2-D flow

$$\tfrac{1}{2} \cdot c_f = \frac{\mathrm{d}\theta}{\mathrm{d}x} + (2+H) \cdot \frac{\theta}{U} \cdot \frac{\mathrm{d}U}{\mathrm{d}x} \tag{7}$$

enables the approximate calculation of c_f, which in this case contains not only the wall shear-stress, but also the pressure drag in the region of separated flow. Directly behind the obstacle, c_f is therefore dramatically increased by the drag of the obstacle itself, then a region of 3-D recirculating flow follows, with vanishing wall shear stress in the flow direction and after that we see the gradual increase of c_f from the laminar to the turbulent level. The fully turbulent level is not quite reached, which is, according to [5], due to the 3-D nature of the flow field behind a single roughness element.
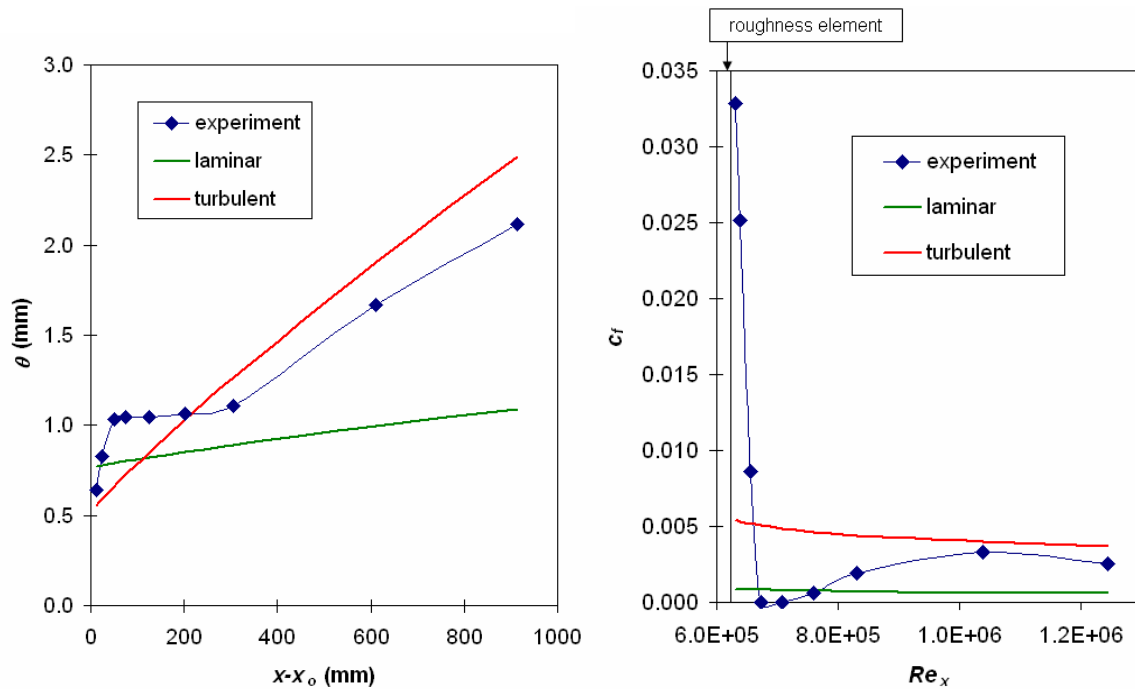
Figure 8. Momentum thickness and calculated friction coefficient from [5] for single roughness element
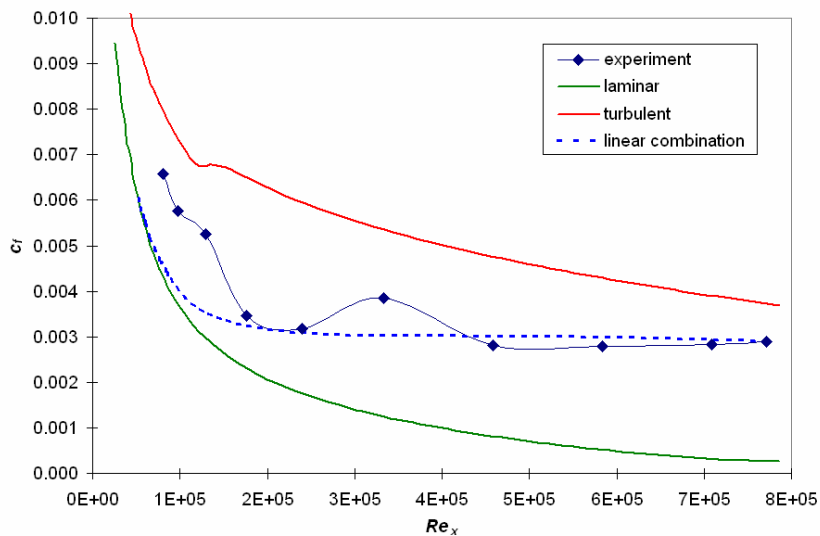
Figure 9. Friction coefficient calculated with momentum equation, data from [7] for roughness strip

Applying the momentum equation 7 to the data of Kerho and Bragg [7] yields c_f as depicted in figure 9. Again the coefficient contains an additional pressure drag directly behind the roughness elements and approximates the skin friction further downstream. There is apparently no region of recirculation as in figure 8. This might be caused by the interference of the many wakes behind several staggered rows of roughness elements. The linear combination method seems to give a good approximation of the wall shear stress. The published intermittency factors in [7] make it possible to compare its growth curve with that of the linear combination factor, as taken from figure 9. Since γ decreases with the distance from the wall, the value directly at the wall is taken for the comparison. The result is depicted in figure 10. As already previously explained, γ and f_{tr} are quite different in the case of a tripped b.l.
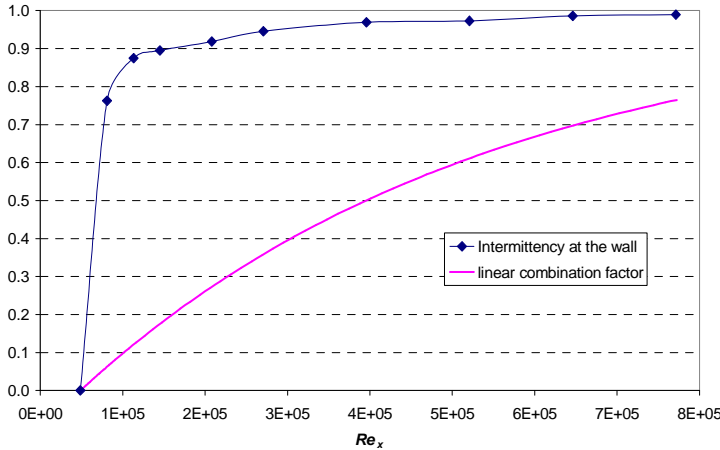
Figure 10. Comparison of intermittency and linear combination factor for NACA 0012 with roughness strip

On the basis of the survey in [18] the following equation is proposed for the determination of the linear combination factor:

$$f_{tr} = 1 - \exp\left[-2.5 \cdot \left(\frac{Re_x - Re_{xo}}{\Delta Re_x}\right)^2\right] \tag{8}$$

The transition length ΔRe_x can be taken from equation 5. For the exponent a value of 2 was chosen, which is debatable. Fransson et al. [17] suggest for natural transition, based on their measurements, an exponent of 3 (Johnson model) whereas in Narasimha's original work the exponent is 2. The best fit to the experimental data for the tripped b.l. at low Tu in figure 9 was achieved with an exponent of 1. The exponent seems to depend on the turbulence level; a final decision can not yet be made. Figure 11 serves to illustrate the quality of the fit of equations 5, 6 and 8 by comparing it to the experimental data of Erm. Most c_f values were measured with a preston tube, the few higher ones were determined with a Clauser chart. $Tu = 0.32$ %.
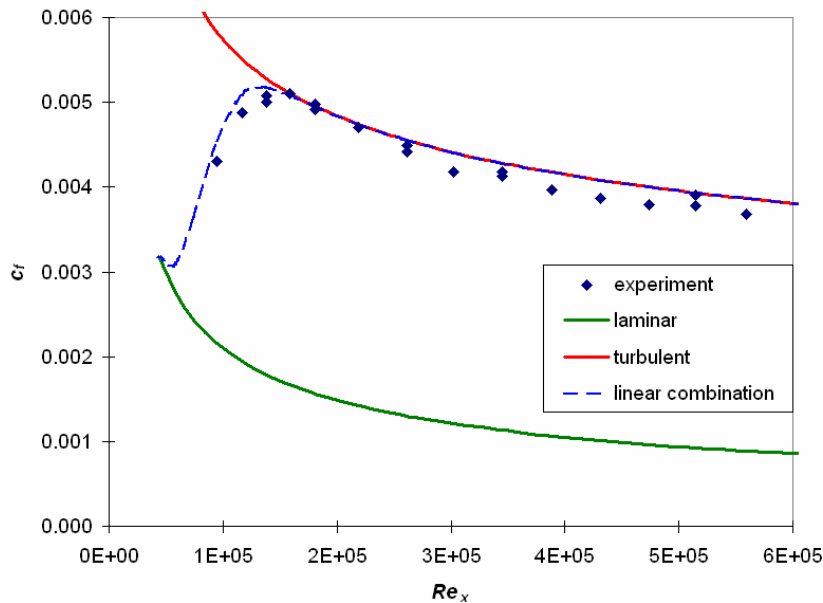
Figure 11. Measured friction coefficients by Erm [15] compared to equation 8, b.l. tripped with a row of pins

4. EXAMPLE CALCULATION FOR THE HULL OF A SAILING YACHT

The equations derived in the previous chapters were incorporated into a computer program that calculates the boundary layer along the ship's hull, using an integral method as described in [25]. With this tool it is possible to calculate the viscous resistance of the models in the Delft-towing-tank. For the turbulence level along the hull a value of 2% was chosen, based on the measurements in [26]. The model Sysser 23 is used here as an example. The b.l. trips of the DSYHS consist of three vertical strips at different distances from the bow. The active strip that causes transition can vary, depending on the Reynolds number. Figure 12 shows the drag area as a function of the Froude number. For the fixed model size the Froude number is proportional to the Reynolds number. The drag area is the resistance force divided by the stagnation pressure. The residuary resistance is determined by subtracting the viscous resistance from the total measured resistance. The viscous resistance curve that is the result of the integral b.l. calculation shows, that the transition point is jumping from the 3rd roughness strip to the 2nd at a Froude number above 0.1. A second jump occurs between 0.2 and 0.25, when the transition point moves from the 2nd to the 1st strip at the bow. These sudden increases in the viscous resistance are also visible in the total measured resistance, whereas the curvature of the residuary resistance is smooth. The viscous resistance calculated by the Delft-method, which uses the ITTC correlation line at $0.7 \cdot L_{WL}$, is also depicted in figure 12. It seems to be a good approximation of the viscous resistance for this model at Fn = 0.25, but is about 20% too large at the lowest speed, because it does not reflect the variation of the transition points.
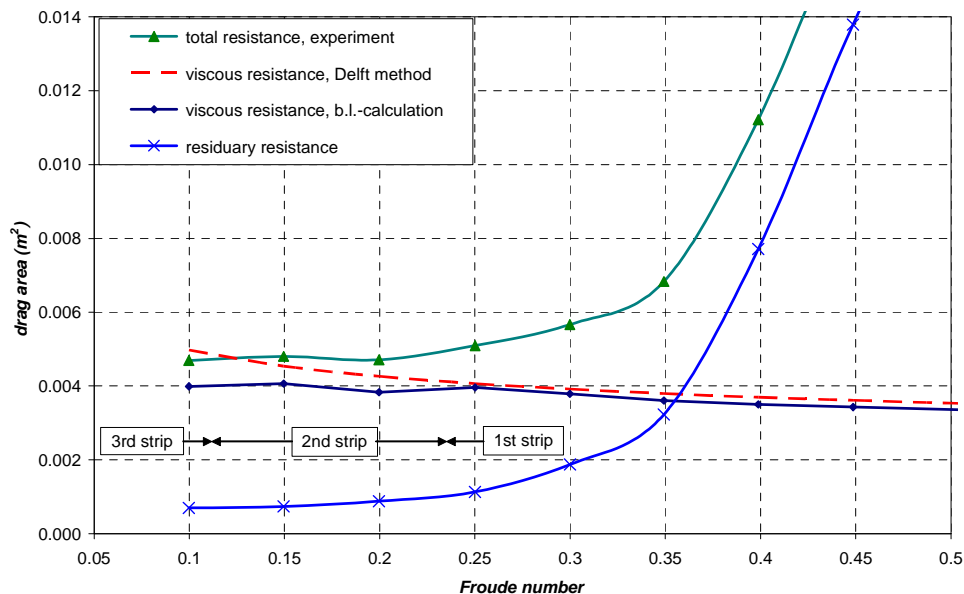
Figure 12. Resistance coefficients for model 23 of the DSYHS

5. CONCLUSION

The equations in this paper that describe the transition caused by a boundary layer trip make it possible to calculate the viscous resistance of a ship model with sand grain strips in the towing tank. For the DSYHS the resulting viscous and residuary resistance gives a more realistic picture at low speeds than the ITTC value that has been the basis of the regression analysis at Delft University.

6. REFERENCES

1. http://dsyhs.tudelft.nl

2. Breslin, J.P., Macovsky, M.S., "Effects of turbulence stimulators on the boundary layer and resistance of a ship model as detected by hot wires", DTMB, Washington, 1950

3. Klebanoff, P.S., Schubauer, G.B., Tidstrom, K.D., "Measurements of the Effect of Two-Dimensional and Three-Dimensional Roughness Elements on Boundary-Layer Transition", *Jour. Aero. Sci.*, Vol. 22, 1955, pp. 803-804

4. Braslow, A.L., Hicks, R.M., Harris, R.V., "Use of grit-type boundary-layer-transition trips on wind-tunnel models", NASA TN D-3579, 1966

5. Klebanoff, P.S., Cleveland, W.G., Tidstrom, K.D., "On the evolution of a turbulent boundary layer induced by a three-dimensional roughness element", *J. Fluid Mech.*, Vol. 237, 1992, pp. 101-187

6. Doenhoff, A.E., Horton, E.A., "A low-speed experimental investigation of the effect of a sandpaper type of roughness on boundary-layer transition", NACA Rep. 1349, 1956

7. Kerho, M.F., Bragg, M.B., "Airfoil Boundary-Layer Development and Transition with Large Leading-Edge Roughness", *AIAA Journal*, Vol. 35, No. 1, 1997

8. Lorenz, M., Schulz, A., Bauer, H.-J., "Predicting Rough Wall Heat Transfer and Skin Friction in Transitional Boundary Layers – A New Correlation for Bypass Transition Onset", *Journal of Turbomachinery*, Vol. 135, 2013

9. Abu-Ghannam, B.J., Shaw, R., "Natural transition of boundary layers – the effects of turbulence, pressure gradient and flow history", *J. Mech. Engng Sci.*, Vol 22, 1980, p.892

10. Fraser, C.J., Higazy, M.G., Milne, J.S., "End-stage boundary layer transition models for engineering calculations", *Proc Instn Mech Engrs, Part C*, Vol. 208, No. 1, 1994, pp. 47-58

11. Drela, M., Youngren, H., XFOIL Computer Program. [Online]. Available: http://web.mit.edu/drela/Public/web/xfoil/

12. Braslow, A.L., Knox, E.C., "Simplified method for determination of critical height of distributed roughness particles for boundary-layer transition at Mach numbers from 0 to 5", NASA TN 4363, 1958

13. Feindt, E.G., "Untersuchungen über die Abhängigkeit des Umschlages laminar-turbulent von der Oberflächenrauhigkeit und der Druckverteilung", *Jahrbuch der Schiffbautechnischen Gesellschaft*, Nr. 50, 1956, pp.180-205

14. Gibbings, J.C., Goksel, O.T., Hall, D.J., "The influence of roughness trips upon boundary-layer transition, Part 3. Characteristics of rows of spherical transition trips", *The Aeronautical Journal*, Vol. 90, 1986, pp. 393-398

15. Erm, L.P., "Low-Reynolds-number turbulent boundary layers", Ph.D. dissertation, Univ. of Melbourne, 1988

16. Smits, A.J., Matheson, N., Joubert, P.N., "Low-Reynolds-number turbulent boundary layers in zero and favorable pressure gradients", *Journal of ship research*, Vol. 27, 1983, pp. 147-157

17. Fransson, J.H.M., Matsubara, M., Alfredsson, P.H., "Transition induced by free-stream turbulence", *J. Fluid Mech.*, Vol. 527, 2005, pp. 1-25

18. Narasimha, R., "Modeling the transitional boundary layer", NASA Contractor Report 187487, 1990

19. Stripf, M., "Einfluss der Oberflächenrauigkeit auf die transitionale Grenzschicht an Gasturbinenschaufeln", Dissertation, Universität Karlsruhe, Germany, 2007

20. Schubauer, G.B., Klebanoff, P.S., "Contributions on the mechanics of boundary-layer transition", NACA Rep. 1289, 1956

21. Fraser, C.J., Gardiner, I.D., Milne, J.S., "A comparison of Two Integral Techniques for the Prediction of Transitional Boundary layer Flow", in *Numerical methods in laminar and turbulent flow*, Vol. 5, Part 2, Swansea, GB: Pineridge Press, 1987, pp. 1712-1724

22. Park, G.I., Wallace, J.M., Wu, X., Moin, P., "Boundary layer turbulence in transitional and developed states", *Physics of Fluids*, Vol. 24, Issue 3, 2012

23. Spalart, P.R., "Direct simulation of a turbulent boundary layer up to $Re_\theta = 1410$", *J. Fluid Mech.*, Vol. 187, 1988, pp. 61-98

24. Stefes, B., "Turbulente Wandgrenzschichten mit und ohne negativen Druckgradienten unter dem Einfluss hoher Turbulenzintensität der Außenströmung", Dissertation, TU Berlin, Germany, 2003

25. Cebeci, T., Cousteix, J., *Modelling and Computation of Boundary-Layer Flows*, Heidelberg, Germany: Springer, 2005

26. Roth, G.I., Mascenik, D.T., Katz, J., "Measurements of the flow structure and turbulence within a ship bow wave", *Physics of Fluids*, Vol. 11, 1999, pp. 3512-3523